JHEP PROCEEDINGS

International Europhysics Conference on HEP

Resonance Production in $\gamma\gamma$ Collisions at L3

Mark Dierckxsens* *On behalf of the L3 Collaboration*

NIKHEF, PO Box 41882, 1009 DB Amsterdam, The Netherlands

E-mail: Mark.Dierckxsens@nikhef.nl

ABSTRACT: An overview is given of a number of resonance production prosesses in two-photon collisions studied with the L3 detector at LEP. The $K^0K^{\pm}\pi^{\mp}$ and $K^0_SK^0_S$ final states are analysed using data collected at centre-of-mass energies up to 202 GeV. The preliminary status of the analyses of the $\pi^+\pi^-\pi^0$ and $\eta\pi^+\pi^-$ channels using all available LEP data is also presented. The contributions from the different spin and helicity states to the signal are determined by comparing the data to the MC prediction. The Q^2-dependence of the differential cross section is studied and the cross section measurement is used to determine the two-photon width times branching fraction. When no signal is observed in the region of a known meson, upper limits on this quantity are derived. Also the possible production of glueball candidates is investigated.

1. Introduction

Resonance production in two photon collisions, $e^+e^- \to e^+e^-\gamma^*\gamma^* \to e^+e^-R$, offers a clean environment to study the spectrum of light mesonic states. Since the outgoing electron and positron are scattered at very small angles, the virtual photons exchanged in the process are quasi real. In this case, the maximum virtuality of the photons, Q^2, can in a good approximation be written as $Q^2 \simeq P_T^2$, where P_T^2 is the square of the sum of the transverse momenta of all the particles in the final state. In such processes, C-even mesons can be produced, which have dominantly spin 0 or 2 at $Q^2 \simeq 0$. It is also possible to form spin 1 particles at higher virtualities.

2. The $\pi^+\pi^-\pi^0$ final state

This preliminary analysis [1] uses the data collected at centre-of-mass energies between 183 GeV and 209 GeV, corresponding to an integrated luminosity of $\mathcal{L} = 682.6$ pb^{-1}.

The events satisfying the requirement of two tracks in the central tracker and two isolated electromagnetic clusters pass the selection. The $\mathrm{d}E/\mathrm{d}x$ measurement of the tracks, originating from the primary vertex, must correspond to the π hypothesis with a confidence

*Speaker.

level C.L.(π) > 10%. The reconstructed mass of the two photons $M(\gamma\gamma)$ has to be between 105 MeV and 165 MeV to be consistent with the π^0 mass.

The cross section is calculated as a function of the effective mass of the three pions $M(\pi^+\pi^-\pi^0)$ and this spectrum, dominated by the $a_2(1320)$, is compared with the one obtained by ARGUS [2] in 1 a). There is in general a good agreement, except for the region just above 1.1 GeV.

A partial wave analysis is performed on the 1998 data, corresponding to $\mathcal{L} = 176.7$ pb^{-1}. This model assumes the production of a resonance with a subsequent two-body decay, $\gamma\gamma \to R \to R'\pi$, with $R' \to \pi\pi$. The resonance R can be a state with $J^P = 0^-, 2^+$ or 2^-, and the intermediated resonances R' considered are the $\rho(770)$, $f_2(1275)$ and the σ-resonance ($f_0(400-1200)$), a parametrisation of the broad component in the S-wave $\pi\pi$-amplitude. A likelihood is constructed from the amplitudes for resonance production, which are parametrised as a sum of Breit-Wigner resonances. An unbinned maximum likelihood fit is then performed to determine the contributions from the various resonances.

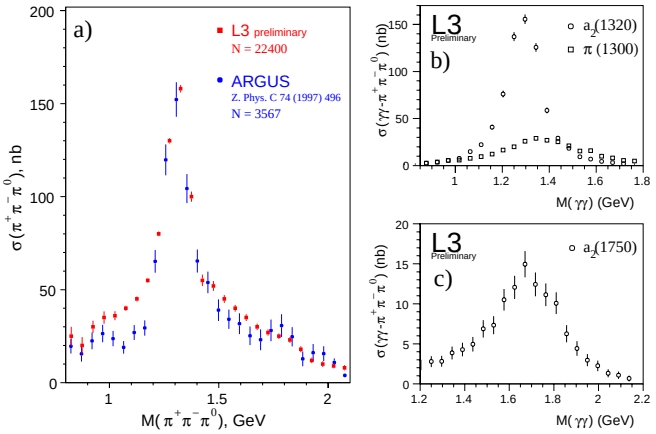

Figure 1: a) Cross section for $\gamma\gamma \to \pi^+\pi^-\pi^0$ compared with the ARGUS [2] results; b) the contributions obtained by the partial wave analysis from the $a_2(1320)$ and the $\pi(1300)$ and c) from the $a_2(1750)$.

Figures 1 b) and c) show the three largest contributions to the cross section. It can be clearly seen that the dominant contribution comes from the $J^{PC} = 2^{++}$ state $a_2(1320)$. In this mass region however, the $J^{PC} = 0^{-+}$ state $\pi(1300)$ needs to be included to have a satisfactory description of the data. In the 1750 MeV mass region, a contributions from the $J^{PC} = 2^{++}$ state $a_2(1750)$ is also found. The fit further improves when the $\pi_2(1670)$ and the $\pi(1800)$, $J^{PC} = 2^{-+}$ and 0^{-+} respectively, are included. This needs to be confirmed by including the data taken at higher centre-of-mass energies.

3. The $\eta\pi^+\pi^-$ final state

The analysis of the events satisfying $P_T^2 < 0.02$ GeV^2 uses the data up to 202 GeV [3], whereas preliminary results using data up to 209 GeV [4] are presented for events with $P_T^2 > 0.02$ GeV^2.

The selection is quite similar as for the $\pi^+\pi^-\pi^0$ channel: events with 2 tracks and 2 photons are selected. However, the mass of the two-photon system is now required to be near the η mass: 0.47 GeV $< M(\gamma\gamma) <$ 0.62 GeV.

The $\eta'(958)$ at threshold and the $f_1(1285)$ peak can clearly be seen in the mass spectrum for all the selected events using the full LEP2 data set (fig. 2 a)). The mass spectrum for events with $P_T^2 < 0.02$ GeV^2 (fig. 2 b)) shows no signal for the $\eta(1440)$ or $\eta(1295)$ so

that 95% C.L. limits can be derived for the $\eta\pi\pi$ decay: $\Gamma_{\gamma\gamma}(\eta(1440)) \times \mathrm{BR}(\eta(1440) \to \eta\pi\pi) < 95$ eV and $\Gamma_{\gamma\gamma}(\eta(1295)) \times \mathrm{BR}(\eta(1295) \to \eta\pi\pi) < 66$ eV.

The data with $P_T^2 > 0.02$ GeV^2 is subdivided into four P_T^2 intervals and each spectrum is fitted with a resonance plus a background function. The measured differential cross section for each P_T^2 interval is fitted with the GaGaRes [5] prediction, containing two parameters. The first one is the gamma-gamma coupling parameter $\tilde{\Gamma}_{\gamma\gamma}$, as defined in [6], and the second is the Λ parameter used to describe the Q^2-dependence in the hard scattering approach [7]. Leaving both Λ and $\tilde{\Gamma}_{\gamma\gamma}$ as free parameters leads to $\Lambda = 1.06 \pm 0.12 \pm 0.09$ MeV and $\tilde{\Gamma}_{\gamma\gamma} = 3.3 \pm 0.6 \pm 1.1$ KeV, where the first error is statistical and the second systematic, with C.L. = 89%. A χ^2 comparison using the approach of the vector dominance model at the ρ-pole [8], gives C.L. $< 10^{-9}$.

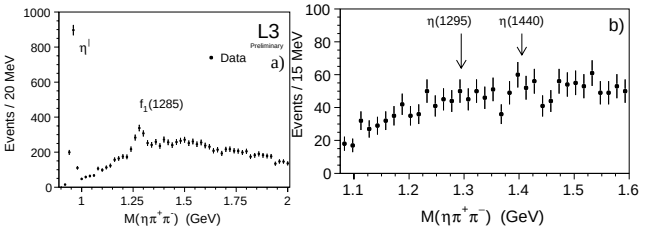

Figure 2: The $\eta\pi^+\pi^-$ mass spectrum a) for the full LEP2 data set and b) in the 1.1 to 1.6 GeV mass region for data up to 202 GeV with $P_T^2 > 0.02$ GeV^2.

4. The $K^0K^\pm\pi^\pm$ final state

The total integrated luminosity of $\mathcal{L}$ =499 pb^{-1} used for this analysis [3] was taken at centre-of-mass energies between 183 GeV and 202 GeV.

Events with four charged particles are selected, from wich two must come from a K_S^0 decaying into $\pi^+\pi^-$ at a secondary vertex. The $\mathrm{d}E/\mathrm{d}x$ measurement of the other two tracks must have a combined confidence level C.L.$(K^\pm\pi^\pm) > 1\%$.

Figures 3 a)-d) show the mass distribution subdivided into 4 P_T^2 intervals. The spectra are fitted with a Gaussian for the signal plus a second order polynomial for the background. Each interval shows a clear signal in the 1440 MeV region which can come from the η and/or the f_1. At higher values of P_T^2, a peak starts to appear between 1.2 and 1.3 GeV, identified with the $f_1(1285)$.

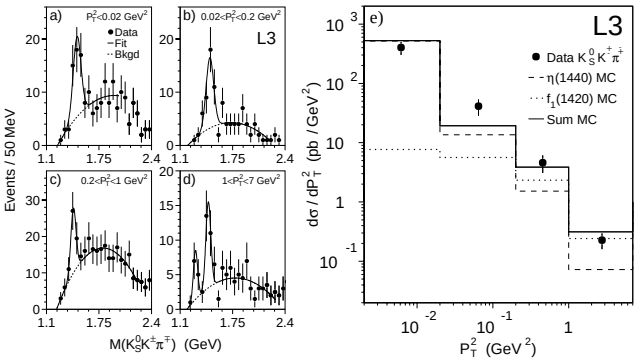

Figure 3: a)-d) The $K^0K^\pm\pi^\pm$ spectrum divided into four different P_T^2 intervals and e) the differential cross section for the 1440 MeV mass region as a function of P_T^2.

In order to determine the different contributions to the 1440 MeV peak region, the differential cross section $\mathrm{d}\sigma/\mathrm{d}P_T^2$ for each P_T^2 interval is calculated and compared to the GaGaRes [5] prediction (fig. 3 b)). Both the hypotheses of a pure pseudoscalar $\eta(1440)$ or a pure axial vector meson $f_1(1420)$ lead to low confidence level values. However, a value of about 9% is obtained if we allow the simultaneous pres-

ence of both mesons. For $P_T^2 < 0.02$ GeV^2, the sample is dominated by the $\eta(1440)$, and from the cross section measurement it follows that $\Gamma_{\gamma\gamma}(\eta(1440)) \times \mathrm{BR}(\eta(1440) \to \mathrm{K\bar{K}}\pi) = 212 \pm 50(\mathrm{stat}) \pm 23(\mathrm{sys})$ eV.

5. The $K_S^0 K_S^0$ final state

For this channel, a total luminosity of $\mathcal{L} = 588$ pb^{-1} is analysed [9], comprising the centre-of-mass energies from 91 GeV up to 202 GeV.

Only events are selected where both kaons decay into two charged pions, originating from a secondary vertex ($K_S^0 K_S^0 \to \pi^+\pi^-\pi^+\pi^-$).

The first of the three peaks seen in the $K_S^0 K_S^0$ mass spectrum (fig. 4) comes from the $f_2(1270)$ and the $a_2(1320)$ tensor mesons and is small due to their destructive interference [10].

The second and largest signal comes from the formation of the $f_2'(1525)$ tensor meson. The polar angle of the two K_S^0's in the two-photon centre-of-mass system is compared to the Monte Carlo prediction in order to determine the spin and helicity composition in the 1400 to 1640 MeV region. Under the hypothesis of a $(J = 0)$ or $(J = 2, \lambda = 0)$ state, the confidence levels are less than 10^{-6}, whereas assuming $(J = 2, \lambda = 2)$ leads to a value of 99.9%. Using the latter assumption, $\Gamma_{\gamma\gamma}(f_2'(1525)) \times BR(f_2' \to \mathrm{K\bar{K}}) = 76 \pm 6 \pm 11$ eV is obtained.

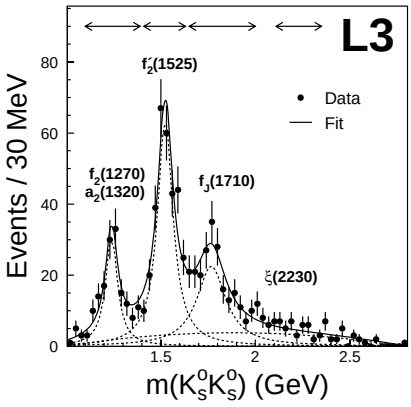

Figure 4: The $K_S^0 K_S^0$ mass spectrum

A similar analysis is performed in the 1640 to 2000 MeV region to measure the spin composition of the $f_J(1710)$. Under the assumption of a pure $(J = 2, \lambda = 2)$ state, a confidence level of 24% is obtained, while including a $(J = 0)$ fraction of 25 ± 16% gives a 68% confidence level and one obtains $\Gamma_{\gamma\gamma}(f_2'(1750)) \times BR(f_2' \to \mathrm{K\bar{K}}) = 49 \pm 11 \pm 13$ eV. The 2^{++} wave may be due to the formation of the first radial excitation of a tensor meson state, while the 0^{++} part may find its origin in a $s\bar{s}$ state.

6. Glueball searches

The two-photon width of gluonium, a bound state of gluons predicted by QCD, is expected to be small since gluons do not couple directly to photons. This is quantified by the stickiness S_R [11], where the radiative width of the J into a resonance R is compared to the two-photon width of this resonance. A large stickiness is expected for a gluon rich state. Another parameter often used is gluiness G_R [12], to quantify the ratio between the two-gluon and two-photon width and is expected to be near unity for a $q\bar{q}$ state.

A good candidate for the ground state tensor glueball is the $\xi(2230)$ since it is produced in a gluon rich environment and its mass is close to the lattice QCD predictions. The $K_S^0 K_S^0$ mass spectrum (fig. 4) does not show any enhancement around the $\xi(2230)$ mass region.

Under the hypothesis of a pure $(J = 2, \lambda = 2)$ state, the upper limit of $\Gamma_{\gamma\gamma}(\xi(2230)) \times BR(\xi \to K^0_S K^0_S) < 1.4$ eV at 95% C.L. is obtained, which results in a lower limit on the stickiness of $S_{\xi(2230)} > 74$. This large value supports the interpretation of the $\xi(2230)$ being a tensor glueball.

Also the $\eta(1440)$ has been suggested as a glueball candidate. From the measurement of the two-photon width $\Gamma_{\gamma\gamma}$ in the $K^0 K^{\pm}\pi^{\pm}$ final state (section 4), the stickiness is determined to be $S_{\eta(1440)} = 79 \pm 26$ and the gluiness $G_{\eta(1440)} = 41 \pm 14$. The upper limit from the $\eta\pi^+\pi^-$ channel (section 3) on $\Gamma_{\gamma\gamma}$ results in the 95% C.L. lower limits $S_{\eta(1440)} > 87$ and $G_{\eta(1440)} > 45$. These values indicate a large gluon admixture of the $\eta(1440)$, but the lattice QCD prediction of the ground state pseudoscalar gluonium is around 2 GeV.

7. Conclusions

Two-photon collisions are a powerful tool to clarify the complex region of low mass resonances. Extensive studies of the production of meson resonances at L3 have improved the measurements of their two-photon widths significantly. Another result is the better description of the Q^2-dependence of the differential cross section. Furthermore, these processes can help to investigate the nature of glueball candidates.

Acknowledgments

I would like to express my gratitude to my colleagues in the L3 collaboration who have helped me preparing this presentation.

References

[1] L3 Coll., M. Acciari *et al.*, L3 note 2677, paper 543 contrib. to the Int. Europh. Conf. on High Energy Physics, Budapest, Hungry (2001).

[2] ARGUS Coll., H. Albrecht *et al.*, Z. Phys **C 74** (1997) 469.

[3] L3 Coll., M. Acciari *et al.*, Phys. Lett. **B 501** (2001) 1.

[4] L3 Coll., M. Acciari *et al.*, L3 note 2677, paper 884 contrib. to the Int. Europh. Conf. on High Energy Physics, Budapest, Hungry (2001).

[5] R. van Gulik, Nucl. Phys. **B 82** (Proc. Suppl.) (2000) 311.

[6] YPC-2γ Coll., H. Aihara *et al.*, Phys. Lett **B 209** (1988) 107; Phys. Rev. **D 38** (1988) 1.

[7] S.J. Brodsky and G.P. Lepage, Phys. Rev. **D 22** (1980) 2157; **D 24** (1981) 1808.

[8] R.N. Cahn, Phys. Rev. **D 35** (1987) 3342; **D 37** (1988) 833.

[9] L3 Coll., M. Acciari *et al.*, Phys. Lett. **B 501** (2001) 173.

[10] H.J. Lipkimn, Nucl. Phys. **B 7** (1968) 321;
D. Faiman *et al.*, Phys. Lett. **B 59** (1975) 269.

[11] M. Chanowitz, Proc. of VI$^{\text{th}}$ Intern. Workshop on Photon-Photon Collisions, Lake Tahoe, California, Ed. R. L. Lander, World Scientific (1985).

[12] F.E. Close, G.R. Farrar, Z. Li, Phys. Rev. **D 55** (1997) 5749;
H.P. Paar, Nucl. Phys. **B 82** (Proc. Suppl.) (2000) 337.